

Estimating and Measuring Thickness of Thin Layers by Monte Carlo Simulation and Backscattered Electron Image Analysis

Joseph Haimovich
Kevin Leibold
Glenn Staudt
AMP Incorporated

ABSTRACT

A fast and inexpensive technique is presented for estimating and, under favorable circumstances measuring, the thickness of thin surface layers. The technique is based on a combination of backscattered electron image analysis with Monte Carlo simulation of the backscatter process. Measurement of backscattered intensity offers an alternative analysis with good counting statistics, spatial resolution, and by means of the accelerating voltage controllable sensitivity. Application of the technique is preferred but not limited to layer thickness ranges from about 0.003 to about 1 μm (0.1 to 40 μinch), depending on the materials. The validity of the technique was verified on specially prepared test samples of tin and gold layers on nickel substrates. Minimum detectable layer thickness in measurements of phase area fractions at the surface of aged tin and tin-lead coatings was estimated. Among applications of current interest discussed here are estimation of the thickness of gold or palladium layers on worn surfaces, estimation of depth of information in cross-sections required to avoid a systematic error, and others.

INTRODUCTION

The surface of the contact spring is the most important factor determining the contact properties, such as contact resistance, friction and wear. Presence of a thin film at the surface can drastically alter some or all of these properties. Considering the

trend of miniaturization of new connector designs, the nature of the surface becomes even more important. Compared to the generally known conventional connectors size, normal force, current, and voltage are drastically reduced.

Frequently, the top surface layer of a contact differs in composition from the rest of the material. Of particular interest are the cases where a thin layer of a metal (e.g. gold, palladium, tin) is applied to a thicker layer of another metal (e.g. nickel, alloys such as palladium-nickel, intermetallic compounds such as copper-tin or nickel-tin). Because of the influence a thin surface layer has on the contact properties, it is highly desirable to be able to measure or at least to reliably estimate the thickness of metallic surface layers down to fractions of a microinch. Often such measurements require high lateral spatial resolution. The commonly used scanning electron microscope (SEM) technique of energy dispersive analysis of X-rays (EDAX) suffers from poor counting statistics at low energy and current, and from diminished spatial resolution at high energy and current. Other techniques for thin layer detection and measurement are available, e.g., Auger and secondary ion mass spectroscopy (SIMS). However, they require specialized, capital intensive instruments which are usually not available in even well equipped general laboratories. Furthermore, if large surface areas on many samples have to be routinely investigated, these techniques are difficult to apply and become prohibitively expensive.

©Copyright 2004 by Tyco Electronics Corporation. All rights reserved.

These disadvantages are avoided by the technique described here. It is a fast and relatively inexpensive technique for estimating and, under favorable circumstances, measuring the thickness of such layers. The technique is based on a combination of backscattered electron image analysis with Monte Carlo simulation of the backscatter process. The measurement of backscattered intensity offers an attractive alternative for scanning electron microscope (SEM) analysis with good counting statistics, good spatial resolution, and controllable sensitivity to layer thickness, which is accomplished by means of the accelerating voltage. In general, the technique is most suitable when the thickness of the surface layer ranges from about 0.01 to about 0.2 μm (about 0.5 to about 10 μinch). The actual ranges depend on layer properties such as average atomic number and density. To verify the validity of the new technique special test samples of tin and of gold on nickel substrates were prepared and exposed to the test. The technique was used to estimate the minimum detectable surface layer thickness in terms of phase area fractions at the surface of aged tin and tin-lead coatings. Other applications included estimating depth of information in cross-sections in order to avoid a systematic error and estimating layer thickness of gold or palladium on worn surfaces.

MONTE CARLO SIMULATION OF ELECTRON BACKSCATTER FROM THIN LAYERS

From a practical, experimental viewpoint backscattered electrons are defined as those that return from the sample with energy greater than about 50 eV. The backscattered electron (BSE) coefficient, η , is defined as the number of backscattered electrons divided by the number of beam electrons incident on the target. Generally, η is found to increase with increasing atomic number, Z ; it is a smooth function of Z ¹. The backscatter coefficient is nearly constant for primary beam voltage in the 10 kV to 50 kV range. Also, the backscatter process is less sensitive to the surface condition and surface texture than secondary electron emission. It should be cautioned, though, that surface roughness will affect the backscattering. A phase with a higher atomic number will generally appear brighter in a backscattered electron (BSE) image. The BSE image then can be used to identify the phase or phases of interest, and to measure the areas occupied by these phases. The BSE image acquisition procedure is relatively fast and allows processing of a large number of images in relatively short time thus ensuring statistically valid results².

Beam electrons penetrate some distance into solid before backscattering; they carry information about the specimen over a range of depth; this range is called *depth of information*¹. If the thickness of a thin layer over a bulk substrate is much greater than this depth, the electrons will be backscattered from the layer only, and the coefficient will be that of the layer material, η_s where the s subscript denotes a layer of saturation thickness. If the thickness of the layer is much less than this depth, the beam electrons will penetrate through it and then backscatter from the underlying substrate; the coefficient, η_0 , will be that of the substrate material. If the thickness of the layer is comparable to the *depth of information*, the backscatter coefficient value will be between the η_0 and the η_s . In this case the back-

scatter coefficient, η_t , becomes a function of the layer thickness, t .

In order to estimate or measure the thickness of thin layers using η_t , one must know how the coefficient varies with the layer thickness, t . This function can be determined either empirically, by measuring η_t in a series of layers of known thickness on a substrate of interest, or theoretically, by calculating η_t as a function of the layer thickness. The second approach is preferred because it avoids time consuming and expensive preparation of a series of standards of well-characterized thickness and composition. Although it is possible to formulate a transport equation describing all scattering in a solid, it may not have a closed-form solution for certain boundary conditions. Monte Carlo simulation provides a practical way for obtaining a description of the electron beam interaction with a solid and can be used to compute η_t ³.

In the study presented here the variation of η_t with the thickness of the top layer was determined by a Monte Carlo simulation of electron scattering. The computer program used was based on a plural scattering Monte Carlo model which is known to be well suited for the case of a thin film over a bulk substrate for accelerating voltages equal or less than 20 kV³. A simulation of 1000 electron trajectories was run 201 times for each value of layer thickness and accelerating voltage for each layer-substrate system being studied. The large number of trajectories was used to decrease the variation in the calculated value of the backscattered fraction of the electrons. In all cases the standard error of the mean of the backscatter fraction was approximately 0.0011, i.e. 0.2% to 0.4% of the η_t value.

The Monte Carlo simulations for tin layers over nickel substrate and for gold layers over nickel substrate were performed for accelerating voltages of 5, 10, 20, and 30 kV. The results for tin are shown in Figure 1, for gold in Figure 2. In both figures the calculated values are represented by the points, the curves fitted to them are represented by a four-parameter sigmoidal curve

$$\eta_t = a_0 + \frac{a_1}{1 + \exp\left(\frac{a_2 - t}{a_3}\right)} \quad (1)$$

which provided the best fit among several candidate expressions. The confidence limits of the fits are shown for 5 kV. Since these limits are very similar at all accelerating voltages, the rest are not shown. This pattern of data presentation is used throughout this paper.

Knowledge of the functional dependence of the backscatter coefficient versus the thickness allows one to estimate or measure the thickness of the top layer simply by estimating or measuring the backscatter coefficient. The thickness can either be calculated using equation (1) or determined graphically from Figures 1 and 2.

The simulations were also performed for other two substrate-layer systems of interest: Sn over Cu_6Sn_5 and Sn over Ni_3Sn_4 .

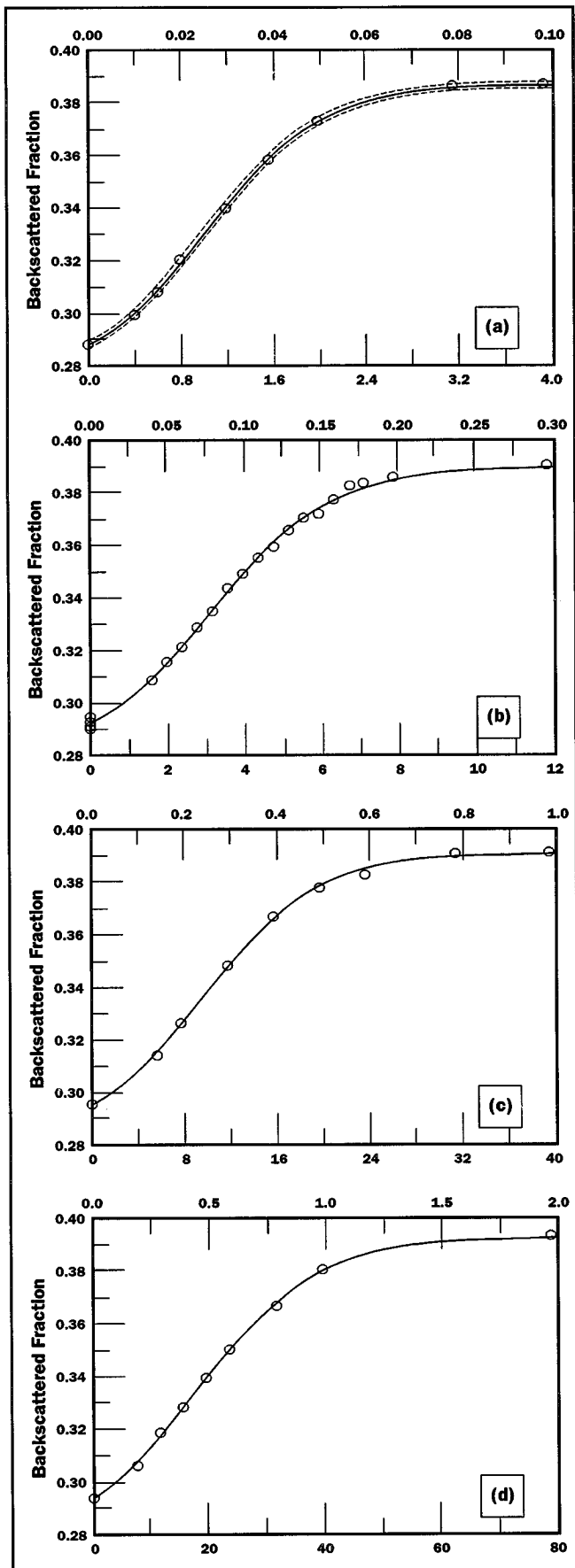


Figure 1. Backscatter coefficient η versus thickness of tin layer on nickel substrate for various values of the accelerating voltage. Upper abscissa in μm , lower abscissa in μinch .—Points are generated by Monte Carlo simulation, curve is sigmoidal fit; the dotted lines are confidence limits of the fit at 95% confidence level.—(a): 5 kV; (b): 10 kV; (c): 20 kV; (d): 30 kV.

For binary alloys or binary intermetallic compounds (IMCs), the effective atomic number was taken to be

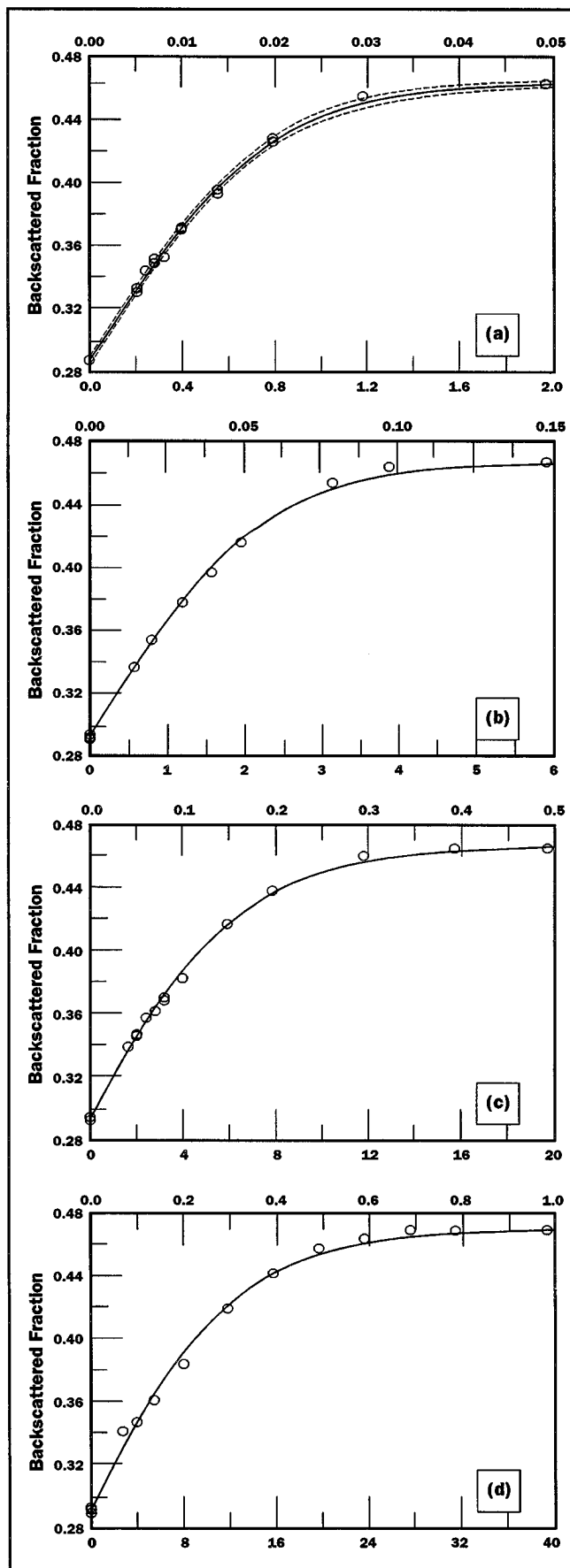
$$Z_{\text{eff}} = \sqrt{cZ_1^2 + (1 - c)Z_2^2} \quad (2)$$

where c is the atomic concentration of component 1, Z_1 and Z_2 are the atomic numbers of components 1 and 2, respectively^{4,5}. The effective atomic number was calculated in this manner for Cu_6Sn_5 and Ni_3Sn_4 . In each system the backscatter coefficient η_t was calculated for a sufficient number of values of layer thickness t . Simulations were performed for the same set of accelerating voltages as above. The results are shown in Figures 3 and 4. As before the calculated values are represented by points, the curves are fitted using equation (1).

EXPERIMENTAL CONFIRMATION OF SIMULATION RESULTS

A SEM is not designed to measure backscatter coefficient η precisely. The collection efficiency differs among commonly used detector systems. Therefore, the exact knowledge of the calculated value of η may not be sufficient, since the observed signal would not be a linear function of η ⁶. For thin layers, the angular distribution of the backscattered electrons is a function of the film thickness⁶. The detector collects only a fraction of backscattered electrons. This fraction lies within the range of backscatter angles characteristic for that particular system. Consequently, the detector's signal depends on the range of the backscatter angles used by the system, i.e., on the detector's geometry. As shown in Figure 5, for the detector used in this work^a the maximum observed fraction of the backscattered electrons is about 25.6% at 10 mm sample-to-detector distance. This fraction was calculated assuming angular distribution of an infinitely thick sample. Under the conditions given above, the detector covers the rather narrow range of scattering angles of 120° to 147° as shown in Figure 6. This narrow range may contribute to deviation from linearity of the observed signal versus the simulated backscatter fraction. The signal of semiconductor and scintillation detectors depends on the energy of the backscattered electrons. Generally, it is proportional to the electron energy. The proportion of high-energy electrons in the backscattered electron spectrum increases with the atomic number Z . Thus, the heavier phases will appear proportionally brighter than expected from the increase in η alone⁴.

^a BSE Detector Amplifier System Model 10-19, LeMont Scientific, Inc., State College, PA.

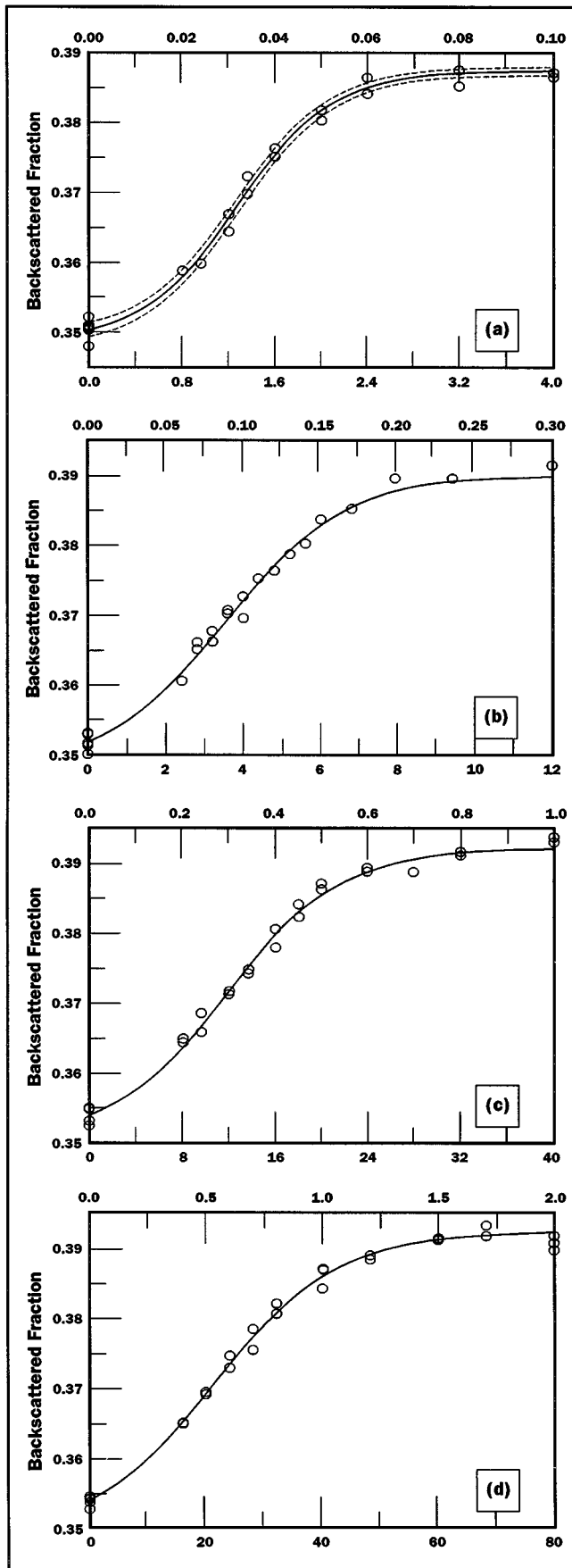


Use of measured backscatter intensities for the analysis of layer thickness would require empirical calibration. Partially due to lack of availability of suitable standards, this is expected to result in time consuming, expensive experimental work. However, if the relative backscatter coefficient with respect to those for bulk samples of the substrate and the coating, as derived from Monte Carlo simulation, are shown to correspond to the relative measured backscatter intensity, thickness values can be inferred from measured intensity data. To demonstrate such a correspondence, several specially designed thin film samples of known thickness were prepared and measured. The two sets of specimens tin and gold, both over nickel substrates, were prepared by electrodeposition. As illustrated in Figure 7 each specimen contained three areas, a thin layer, the bare substrate, and a layer of saturation thickness. The samples were designed so that all three areas would be present on a BSE SEM image of a sample, thus making them suitable for image analysis. Each thin layer thickness was measured at 50 separate points by X-ray fluorescence calibrated with standards of known thickness. The points were selected near the area where the three regions converge. Since the layers were very thin, 50 similar measurements were taken on the uncoated region for precise substrate correction. These thicknesses are given in Tables 1 to 4, assuming densities of 7.3 g/cm^3 for tin and 17.5 g/cm^3 for cobalt-hardened gold.

The coatings were deposited from bright plating baths onto polished substrates to yield smooth surfaces. This was done to lessen the effect of the surface topography on the experimental results. Although much less sensitive to surface features than that of secondary electrons, the intensity of backscattered electrons depends strongly on surface roughness. In fact, a thick, i.e., saturation layer of matte tin that has a very rough surface yielded a backscatter intensity that was less than that obtained from a thin layer of matte tin over smooth nickel substrate. This could be attributed to the greater surface roughness of the much thicker saturation coating.

The backscattered images of the samples were acquired with an AMRAY 1000 SEM at 10 mm sample-to-detector distance and a magnification of 50X. Accelerating voltages were 30, 20, 10, and 5 kV. Typical backscattered images are shown in Figure 8. The brightness, i.e. the signal intensity from the thin layer lies between that of the bare substrate and the infinitely thick layer. Figure 8 also shows the pixel intensity histograms superimposed onto the backscatter images. The left peak corresponds to the bare substrate area, the peak on the right represents the thick, saturation thickness layer, the central peak corresponds to the thin layer. The histogram has 256 levels because of the 8-bit conversion of the analog intensity signal. In most cases this

Figure 2. Backscatter coefficient η versus thickness of gold layer on nickel substrate for various values of the accelerating voltage. Upper abscissa in μm , lower abscissa in μinch .—Points are generated by Monte Carlo simulation, curve is sigmoidal fit; the dotted lines are confidence limits of the fit at 95% confidence level.—(a): 5 kV; (b): 10 kV; (c): 20 kV; (d): 30 kV.



number of levels provides for sufficiently high resolution. Gain of the BSE detector amplifier and image brightness and contrast were adjusted to maximize the separation between the substrate peak and the thick layer peak, thus providing the best resolution for the position of the thin layer peak.

The normalized thin layer peak position on the pixel intensity histogram can be defined as

$$P_t = \frac{(I_t - I_0)}{(I_s - I_0)} \quad (3)$$

where I_t is the position of the thin layer peak, I_0 that of the substrate peak, and I_s that of the thick layer peak. Assuming that the backscatter coefficient of the thin layer is linear with the layer's normalized position, P_t , the backscatter coefficient of the thin layer is

$$\eta_t = \eta_0 + P_t(\eta_s - \eta_0). \quad (4)$$

The layer can then be calculated using equation (1) with the constants obtained by Monte Carlo simulation

$$t_m = a_2 - a_3 \cdot \ln\left(\frac{a_1}{\eta_t - a_0} - 1\right) \quad (5)$$

The results of the measurements at 10 mm sample-to-detector distance are given in Table 1 for tin and Table 2 for gold. For tin samples some of the measurements were repeated two to three times. Since no significant variations were observed, only the averages are given in Table 1.

The measurements at 20 kV were repeated at the largest available sample-to-detector distance of 22 mm. This was done to vary the backscatter angles to determine the effect of angular distribution: the backscatter angle range in this case is 142° to 163° . The results of these measurements are given in Table 3 for tin and Table 4 for gold. They are nearly identical to those obtained at 10 mm distance and a corresponding angle range of 120° to 147° . Thus, the normalized peak position is not a function of the sample-to-detector distance in 10 mm to 22 mm range.

The thickness, t_m , of the test samples obtained by the combination of Monte Carlo simulation and image analysis of backscattered images, further referred to as MCS/BSEIA, are higher than the thickness values, t_x , measured by X-ray fluorescence. To illustrate this difference, the ratios $R = t_m/t_x$ are entered in the last columns of Tables 1 through 4. For tin this ratio ranges from 1.6 to 2.7, the weighted average and associ-

Figure 3. Backscatter coefficient η versus thickness of tin layer on Cu_6Sn_5 IMC substrate for various values of the accelerating voltage. Upper abscissa in μm , lower abscissa in μinch .—Points are generated by Monte Carlo simulation, curve is sigmoidal fit; the dotted lines are confidence limits of the fit at 95% confidence level.—(a): 5 kV; (b): 10 kV; (c): 20 kV; (d): 30 kV.

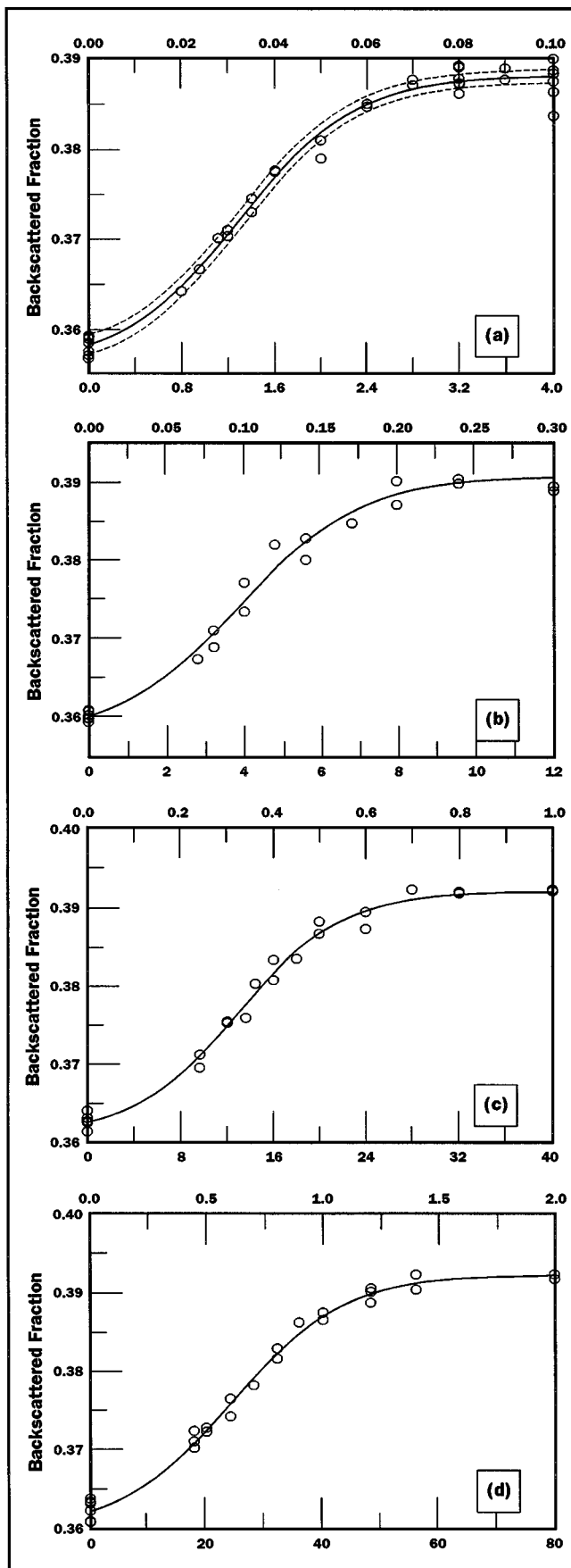


Figure 4. Backscatter coefficient η versus thickness of tin layer on Ni_3Sn_4 IMC substrate for various values of the accelerating voltage. Upper abscissa in μm , lower abscissa in μinch .—Points are generated by Monte Carlo simulation, curve is sigmoidal fit; the dotted lines are confidence limits of the fit at 95% confidence level.—(a): 5 kV; (b): 10 kV; (c): 20 kV; (d): 30 kV.

ated standard deviation are 1.99 and 0.04, respectively. For gold it is $1.1 \leq R \leq 1.6$, weighted average and standard deviation are 1.47 and 0.03. Since the MCS/BSEIA thicknesses

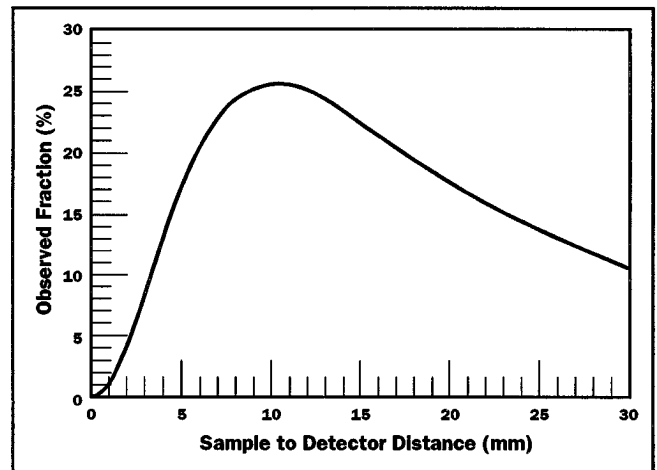


Figure 5. Fraction of BSE electrons arriving at the BSE detector versus sample to detector distance (LeMont Scientific detector). The calculations assumed the angular electron distribution of a bulk material.

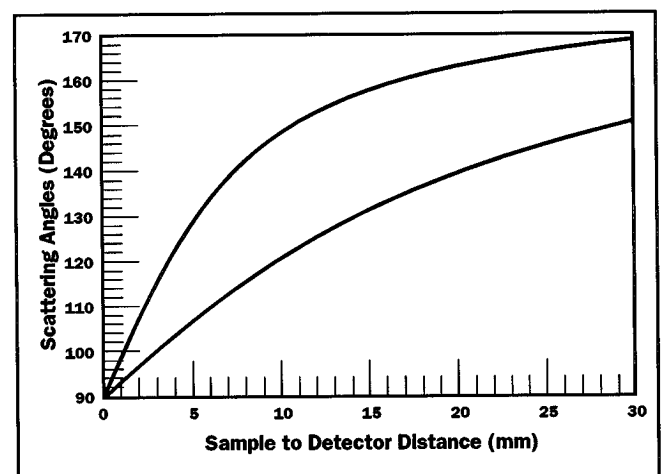


Figure 6. Minimum and maximum backscatter angles versus sample to detector distance (LeMont Scientific BSE detector).

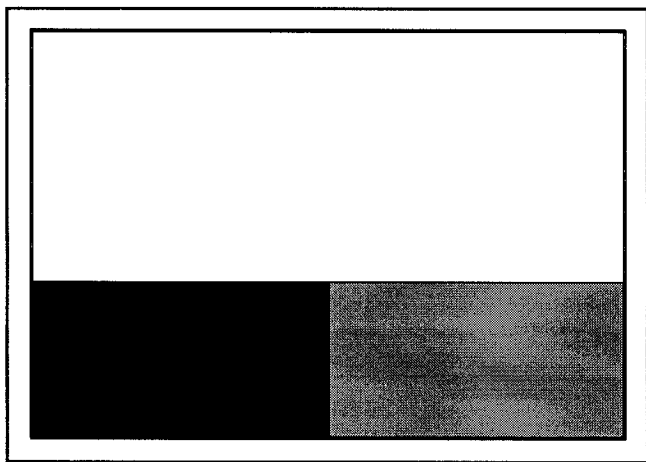


Figure 7. Diagram of MCS/BSEIA test sample: top (white)—thick (bulk) layer; bottom right (gray)—thin layer; bottom left (black)—substrate.

differ from the values determined by X-ray fluorescence, use of the method described here requires calibration. However, if the bias in the MCS/BSEIA is consistent, limited calibration may be practical.

To ascertain consistency of the bias in the thickness values from the MCS/BSEIA method, it is necessary to analyze the uncertainties associated with the measurements. For the characterization of the layer thickness, the uncertainty was estimated from X-ray fluorescence data and associated instrumental parameters⁷. Since the areas analyzed by X-ray fluorescence and by electron backscatter were not identical, the observed distribution of thickness over the sampled area was taken as a direct component of the total uncertainty. Uncertainty of the X-ray calibration was taken as the usual certified tolerance of the calibration standards, i.e., $\pm 5\%$ at the 95% confidence level. Uncertainty of the relative electron backscatter intensity from image analysis was estimated by assuming a single pixel standard deviation in the determination of peak positions. In addition to the effect of the standard fit error the corresponding uncertainty in the backscatter coefficient, assuming exact values of the coefficients for the bulk elements, was propagated to a thickness uncertainty through the fit of the Monte Carlo simulation results.

The thickness ratios R are plotted in Figure 9 for tin on nickel, in Figure 10 for gold on nickel. The estimated uncertainties at the 95% confidence level and the overall weighted average ratio are included in the diagrams. Although some trends of the R with thickness appear in the plots, the 95% confidence limits fail to encompass the overall weighted average for only one of the 31 experiments. This is within statistical expectation and is consistent with a constant bias in the MCS/BSEIA thickness for a specific coating material. Consequently, the MCS/BSEIA technique can be applied to coating layer thickness determination by calibration with a single standard to establish the thickness ratio.

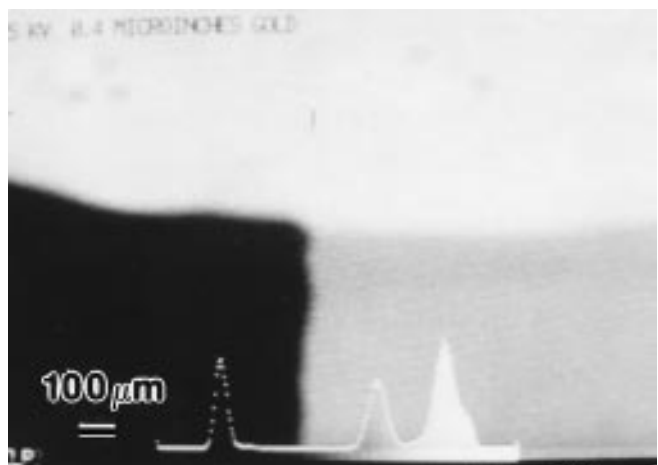
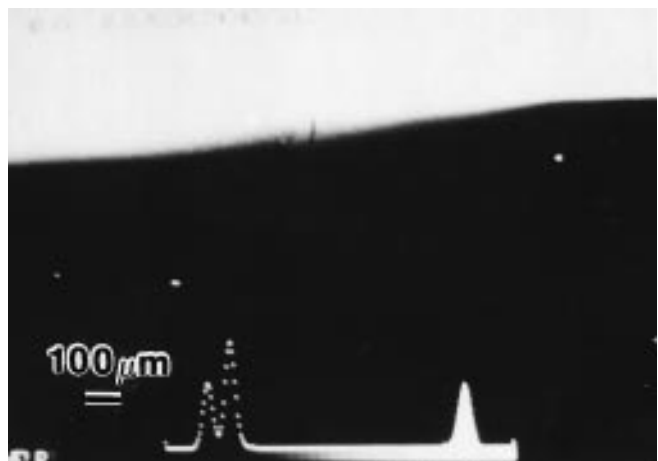
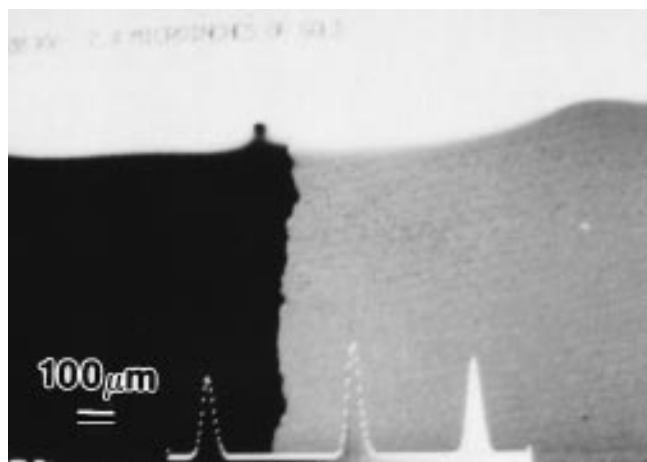


Figure 8. BSE image for three values of the acceleration voltage and gold layer thickness of a MCS/BSEIA test sample. Gold on nickel, with the pixel brightness distribution histogram superimposed. Top—thick (bulk) gold layer, bottom right—thin gold layer, bottom left—nickel substrate. Magnification 50X.—(a): 20 kV, gold layer thickness— $0.065 \mu\text{m}$ (2.6 microinch). (b): 30 kV, gold layer thickness— $0.022 \mu\text{m}$ (0.86 microinch). (c): 5 kV, gold layer thickness— $0.012 \mu\text{m}$ (0.46 microinch).

Table 1. Tin Test Samples, Results of Thickness Measurements, X-ray and BSE Image Analysis/Monte Carlo Simulation. Sample-to-Detector Distance 10 mm (Working Distance 12 mm).—First column by X-ray, fourth column by MCS/BSEIA.

Thickness $t_x \pm s$ [μm]	Normalized Peak Position P_t	Backscatter Coefficient ν_t	Thickness $t_m \pm s$ [μm]	Ratio $(t_m/t_x) \pm s$
Accelerating Voltage 30 kV				
0.060 \pm 0.003	0.059	0.297	0.094 \pm 0.017	1.57 \pm 0.30
0.080 \pm 0.006	0.116	0.303	0.167 \pm 0.014	2.09 \pm 0.24
0.140 \pm 0.007	0.227	0.314	0.288 \pm 0.011	2.06 \pm 0.13
0.178 \pm 0.010	0.302	0.322	0.361 \pm 0.011	2.03 \pm 0.13
0.379 \pm 0.020	0.637	0.357	0.673 \pm 0.013	1.78 \pm 0.10
Accelerating Voltage 20 kV				
0.017 \pm 0.002	0.044	0.295	0.039 \pm 0.013	2.35 \pm 0.87
0.060 \pm 0.003	0.205	0.312	0.140 \pm 0.007	2.33 \pm 0.18
0.080 \pm 0.006	0.283	0.319	0.178 \pm 0.006	2.22 \pm 0.19
0.140 \pm 0.007	0.491	0.340	0.270 \pm 0.006	1.93 \pm 0.10
0.178 \pm 0.010	0.629	0.354	0.333 \pm 0.007	1.87 \pm 0.11
Accelerating Voltage 10 kV				
0.017 \pm 0.002	0.204	0.312	0.044 \pm 0.002	2.68 \pm 0.40
0.060 \pm 0.003	0.696	0.36	0.118 \pm 0.003	1.97 \pm 0.12
0.080 \pm 0.006	0.799	0.37	0.139 \pm 0.003	1.73 \pm 0.14
Accelerating Voltage 5 kV				
0.017 \pm 0.002	0.743	0.362	0.041 \pm 0.001	2.48 \pm 0.35

Table 2. Gold Test Samples, Results of Thickness Measurements, X-ray and BSE Image Analysis/Monte Carlo Simulation. Sample-to-Detector Distance 10 mm (Working Distance 12 mm).—First column by X-ray, fourth column by MCS/BSEIA.

Thickness $t_x \pm s$ [μm]	Normalized Peak Position P_t	Backscatter Coefficient η_t	Thickness $t_m \pm s$ [μm]	Ratio $(t_m/t_x) \pm s$
Accelerating Voltage 30 kV				
0.012 \pm 0.002	0.040	0.301	0.013 \pm 0.008	1.10 \pm 0.72
0.022 \pm 0.001	0.084	0.309	0.027 \pm 0.008	1.24 \pm 0.37
0.043 \pm 0.001	0.171	0.324	0.055 \pm 0.008	1.28 \pm 0.19
0.066 \pm 0.003	0.282	0.344	0.093 \pm 0.009	1.41 \pm 0.14
0.091 \pm 0.003	0.381	0.362	0.129 \pm 0.009	1.41 \pm 0.11
0.127 \pm 0.004	0.528	0.387	0.189 \pm 0.011	1.49 \pm 0.10
0.211 \pm 0.007	0.755	0.428	0.319 \pm 0.019	1.52 \pm 0.10
Accelerating Voltage 20 kV				
0.012 \pm 0.002	0.078	0.308	0.012 \pm 0.003	1.06 \pm 0.32
0.022 \pm 0.001	0.182	0.326	0.029 \pm 0.003	1.35 \pm 0.14
0.043 \pm 0.001	0.352	0.355	0.060 \pm 0.003	1.39 \pm 0.09
0.66 \pm 0.003	0.542	0.388	0.101 \pm 0.004	1.53 \pm 0.09
0.091 \pm 0.003	0.665	0.410	0.135 \pm 0.005	1.47 \pm 0.08
0.127 \pm 0.004	0.818	0.436	0.196 \pm 0.009	1.54 \pm 0.09
Accelerating Voltage 10 kV				
0.012 \pm 0.002	0.277	0.342	0.017 \pm 0.001	1.43 \pm 0.32
0.022 \pm 0.001	0.546	0.388	0.034 \pm 0.001	1.57 \pm 0.09
0.043 \pm 0.001	0.810	0.435	0.062 \pm 0.003	1.44 \pm 0.08
Accelerating Voltage 5 kV				
0.012 \pm 0.002	0.682	0.407	0.016 \pm 0.001	1.35 \pm 0.29

Table 3. Tin Test Samples, Results of Thickness Measurements, X-ray and BSE Image Analysis/Monte Carlo Simulation. Sample-to-Detector Distance 22 mm (Working Distance 24 mm). Accelerating Voltage 20 kV.—First column by X-ray, fourth column by MCS/BSEIA.

Thickness $t_x \pm s$ [μm]	Normalized Peak Position P_t	Backscatter Coefficient ν_t	Thickness $t_m \pm s$ [μm]	Ratio $(t_m/t_x) \pm s$
0.017 \pm 0.002	0.053	0.299	0.046 \pm 0.012	2.80 \pm 0.82
0.060 \pm 0.003	0.189	0.312	0.131 \pm 0.008	2.19 \pm 0.18
0.080 \pm 0.006	0.271	0.320	0.172 \pm 0.007	1.98 \pm 0.11
0.140 \pm 0.007	0.509	0.344	0.278 \pm 0.007	1.98 \pm 0.11
0.178 \pm 0.010	0.573	0.350	0.306 \pm 0.007	1.72 \pm 0.11

ESTIMATING MINIMUM RESOLVABLE THICKNESS: TIN OVER INTERMETALLIC COMPOUND

This section describes the application of the MCS/BSEIA technique to measurement of residual free tin in aged samples of tin over copper alloys and over nickel. Some typical backscatter images of aged tin over copper alloy and of aged tin over nickel underplating are shown in Figures 11 and 12. The light phase is tin, and the dark phase is intermetallic compound (IMC). Such images were used to estimate the surface fractions occupied by tin and by IMC. The brightness of the tin phase in the image is a function of its thickness. The thinner the tin layer, the darker it will appear in the BSE image. A very thin tin layer might not appear bright enough to be distinguished from the underlying IMC. Because some of the tin phase at the surface of the aged samples might be very thin, an estimate is needed for the minimum thickness of a tin layer that can be resolved, i.e., can be unambiguously distinguished from the IMC. If this estimate is small, the surface fractions measured by the BSE image analysis will be close to the true values, since only very thin areas of tin will be confused with IMC.

This minimum resolvable thickness can be estimated using the η_t vs. t curves of Figures 3 and 4. For the thickness of a layer to be observed by MCS/BSEIA, its peak in the intensity histo-

Table 4. Gold Test Samples, Results of Thickness Measurements, X-ray and BSE Image Analysis/Monte Carlo Simulation. Sample-to-Detector Distance 22 mm (Working Distance 24 mm). Accelerating Voltage 20 kV.—First column by X-ray, fourth column by MCS/BSEIA.

Thickness $t_x \pm s$ [μm]	Normalized Peak Position P_t	Backscatter Coefficient η_t	Thickness $t_m \pm s$ [μm]	Ratio $(t_m/t_x) \pm s$
0.012 \pm 0.002	0.085	0.309	0.013 \pm 0.003	1.16 \pm 0.35
0.022 \pm 0.001	0.174	0.325	0.028 \pm 0.003	1.29 \pm 0.15
0.043 \pm 0.001	0.313	0.349	0.053 \pm 0.003	1.22 \pm 0.08
0.066 \pm 0.003	0.500	0.381	0.091 \pm 0.004	1.38 \pm 0.08
0.091 \pm 0.003	0.639	0.405	0.128 \pm 0.005	1.39 \pm 0.07
0.127 \pm 0.004	0.821	0.437	0.198 \pm 0.009	1.56 \pm 0.09

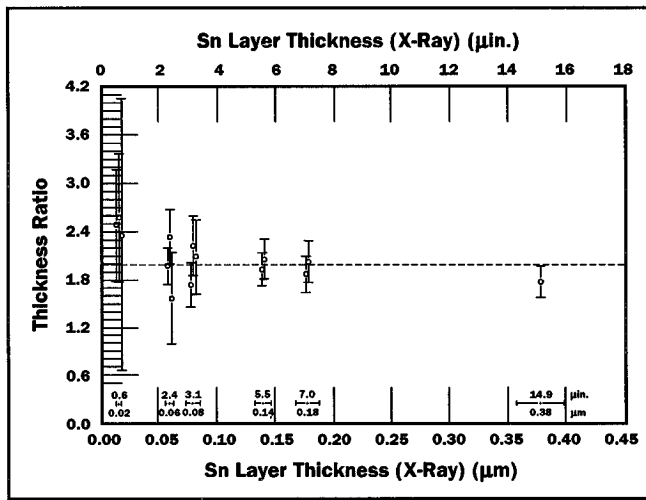


Figure 9. Thickness ratio t_m/t_x for tin layers on nickel substrate plotted as function of the tin layer thickness. Vertical error bars are estimated uncertainties at 95% confidence level; dotted line is the overall, weighted average ratio. Horizontal error bars are one standard deviation of t_x . Ratios for the same thickness t_x are offset for clarity.

gram must be separated from that of a bulk material. Overlapping peaks are expected to be resolvable when separated by approximately three standard deviations. Since the observed standard deviations of the relative peak positions for tin are approximately 0.01, resolution of a thin layer of tin from a nickel substrate requires a relative peak position of approximately 0.03 minimum. In case of tin over IMC, the difference in the backscatter coefficients between the bulk materials is approximately three times less than that for tin over nickel; consequently, the uncertainty in the relative peak posi-

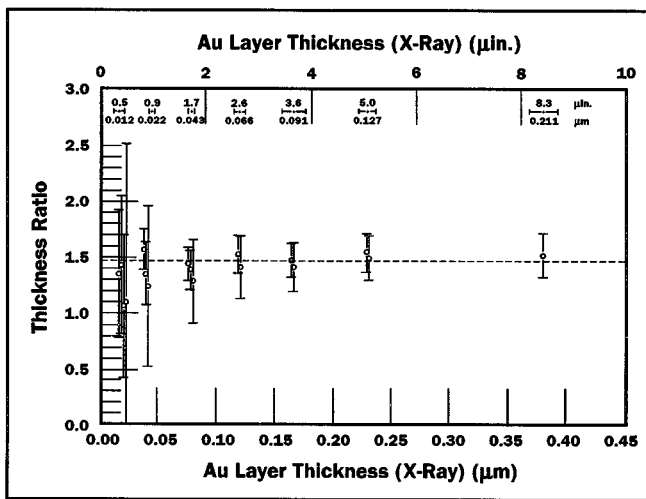


Figure 10. Same as Figure 9 but for gold layers on nickel substrate.

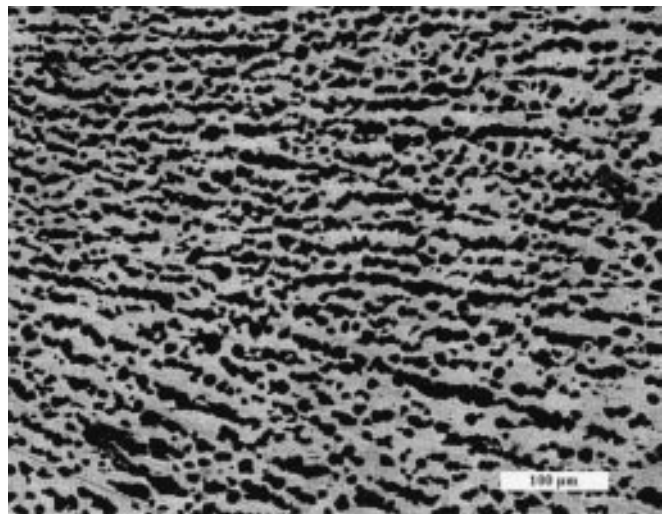


Figure 11. Backscatter SEM image acquired and stored by image analysis system. Sample: hot air leveled tin over phosphor bronze. Aged 2000 hours at 125°C. Light phase—tin, dark phase— Cu_6Sn_5 IMC. Magnification 200X.

tion is expected to be approximately three times larger, i.e., about 0.1. Considering the case of tin over Cu_6Sn_5 at 10 kV shown in Figure 3b, this resolution limit corresponds to a tin thickness of approximately 0.03 μm (1.2 μinch). Anything below that point can be considered to belong to the IMC phase, anything above can be assigned to the tin phase. For the lower accelerating voltage of 5 kV in Figure 3a, this value is about 0.013 μm (0.5 μinch). Corresponding values for the case of tin over Ni_3Sn_4 are approximately 0.013 μm (0.5 μinch) for 5 kV,

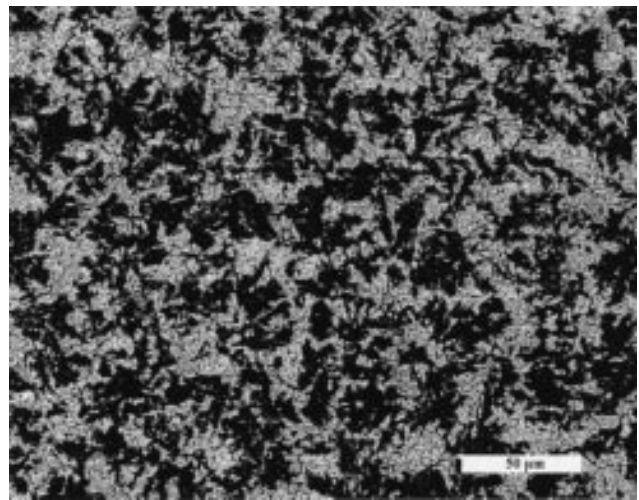


Figure 12. Backscatter SEM image acquired and stored by image analysis system. Sample: electroplated matte tin over nickel underplating over brass. Aged 4000 hours at 125°C. Light phase—tin, dark phase— Ni_3Sn_4 IMC. Magnification 500X.

Figure 4a, and approximately 0.04 μm (1.4 μinch) for 10 kV, Figure 4b. Thus, the thickness of tin that would be confused with bare IMC is rather small. Therefore, this measurement effectively represents the tin area fraction corresponding to the tin thickness at and above the intensity discrimination level. The minimum resolvable thickness is further reduced by applying the empirical correction factor, which for tin over nickel is about 2. With the correction, the minimum observable thickness is about 0.02 μm (0.7 μinch) at 10 kV, and about 0.006 μm = 6 nm (0.24 μinch) at 5 kV.

ESTIMATING AND MEASURING THICKNESS OF THIN LAYERS

The estimate of minimum resolvable thickness described above is one application of MCS/BSEIA. This technique can also be used for experimental determination of the layer thickness. It can be applied in a straightforward way if the samples are similar to the test specimens described above, i.e., if all three areas of interest can be made to appear in the same BSE image. These areas are the bare substrate, the thin layer being measured, and a layer of saturation thickness of the same composition. The normalized backscatter intensity of the thin layer can then be used to calculate the layer thickness from the relationship η_t versus t obtained by Monte Carlo simulation. The Monte Carlo results can be used directly to find a rough estimate of the layer thickness. The results can be refined by applying an empirical correction factor based on calibration with a standard of known thickness.

The example discussed above is most suitable for the technique. However, most samples will not conform to this configuration. Other contrast producing configurations are more likely to occur. Some of them are

- a thin layer and bare substrate,
- a thin layer and a thick layer assumed to be of infinite thickness,
- two or more thin layers of different thicknesses.

In none of these situations is it possible to determine directly the normalized peak position of the layer or layers of interest because at least one of the reference areas is missing. In these cases it is still possible to estimate the thickness of the layers using the dependence of the backscatter process on the electron beam energy. This is illustrated in Figure 13 using the results of a simulation for a gold layer on nickel. With increasing beam energy the curves shift to the right to higher thickness. In order to produce BSE contrast for a nickel substrate, the minimum backscatter coefficient, η_{\min} , of a thin layer of gold must be

$$\eta_{\min} = \eta_0 + c_{\min}(\eta_s - \eta_0). \quad (6)$$

Similarly, to produce sufficiently high contrast with an infinitely thick layer, η_t must be less than

$$\eta_{\max} = \eta_0 + c_{\max}(\eta_s - \eta_0). \quad (7)$$

As mentioned in the previous section, the actual limits of resolution, $\Delta\eta$, will depend on instrumental capabilities but also on the materials, i.e., the magnitude of the difference in backscatter coefficients. For gold on a nickel substrate $\Delta\eta(\text{Au/Ni})$ is 0.174 in the 5 to 30 kV range, for tin on nickel $\Delta\eta(\text{Sn/Ni})$ is 0.099, and for tin on IMC $\Delta\eta(\text{Sn/IMC})$ is considerably less. From the observations on gold and tin, reasonable estimates of c_{\min} are 0.02 for gold and nickel, 0.03 for tin and nickel, and 0.1 for tin and IMC. The values of η_{\min} and η_{\max} correspond to thicknesses t_{\min} and t_{\max} . At any given beam energy expressed in terms of the accelerating voltage V , layers thinner than $t_{\min}(V)$ will be indistinguishable from the substrate. Layers thicker than $t_{\max}(V)$ will be indistinguishable from the infinitely thick layer.

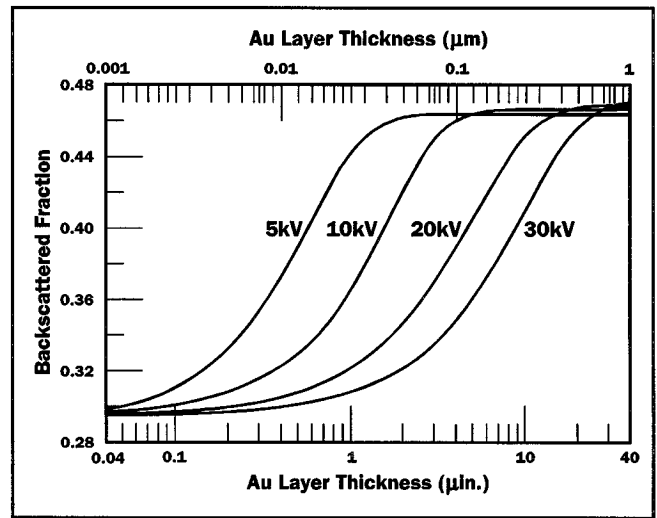


Figure 13. Backscatter coefficient η versus thickness of gold layer on nickel substrate, combined plot for 5 kV to 30 kV accelerating voltage range. The curves are sigmoidal fits to the simulated points.

For gold over nickel t_{\min} and t_{\max} are plotted versus accelerating voltage V in Figure 14. The thickness values obtained by Monte Carlo simulation were corrected using a factor of 1.47. From the variation of t_{\min} and t_{\max} with V , limits on the thickness of the layer can be estimated. For example, using the t_{\max} curve, a 0.1 μm (4 μinch) thick layer of gold on nickel will be distinguishable from an infinitely thick layer at 20 kV and higher, but not at 10 kV and below. Using the t_{\min} curve a layer that is 0.001 μm = 1 nm (0.04 μinch) thick will be distinguishable from the substrate at 10 kV and below, but not at 20 kV and above. Thus, the thickness of layers ranging from about 0.0003 to about 0.5 μm (0.01 to 20 μinch) can be estimated using Figure 14. A similar plot for tin over nickel is given in Figure 15. It is $c_{\min}=0.03$ and $c_{\max}=0.97$. The thickness values are corrected using a factor of 1.99. In this case the range of thicknesses that can be estimated is from about 0.0015 to about 0.7 μm (0.06 to 30 μinch).

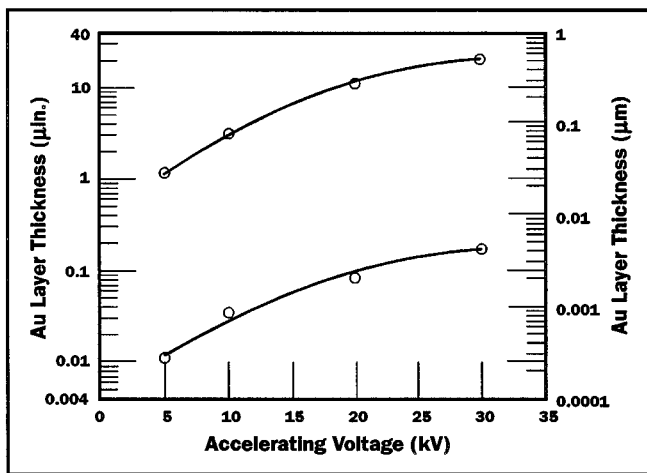


Figure 14. MCS/BSEIA detection limit, t_{min} , and saturation limit, t_{max} , versus accelerating voltage, for gold layer on nickel substrate.

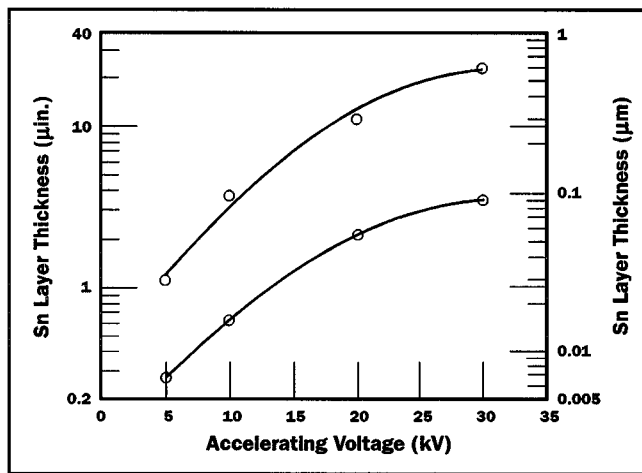


Figure 16. MCS/BSEIA detection limit, t_{min} , and saturation limit, t_{max} , versus accelerating voltage, for tin layer on Cu_6Sn_5 substrate.

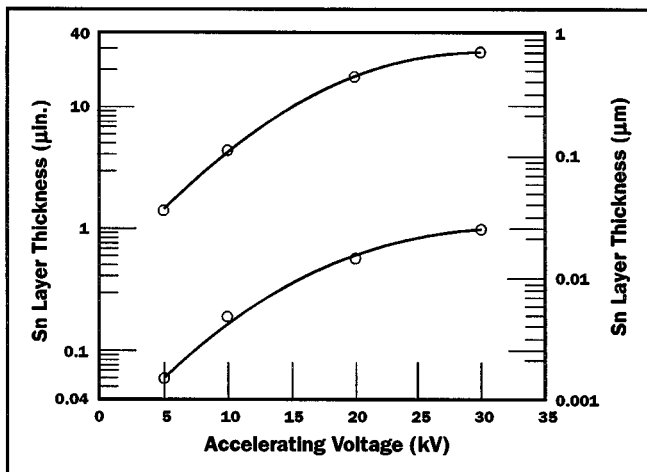


Figure 15. MCS/BSEIA detection limit, t_{min} , and saturation limit, t_{max} , versus accelerating voltage, for tin layer on nickel substrate.

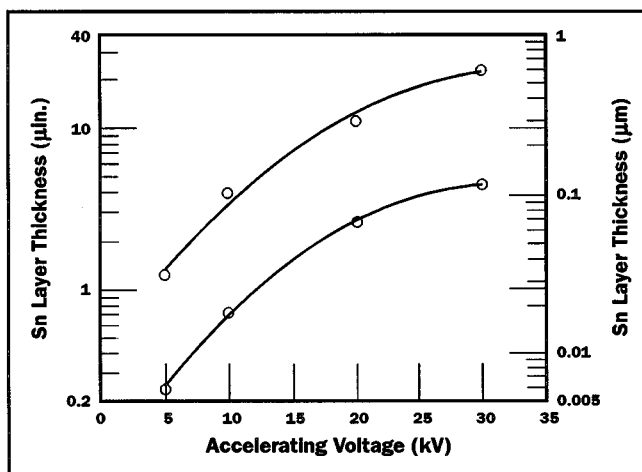


Figure 17. MCS/BSEIA detection limit, t_{min} , and saturation limit, t_{max} , versus accelerating voltage, for tin layer on Ni_3Sn_4 substrate.

A plot of t_{min} and t_{max} versus voltage for tin over Cu_6Sn_5 is given in Figure 16. The limit in this case was assumed to be 10% of $\Delta\eta(Sn/Cu_6Sn_5)$, i.e., $c_{min}=0.1$, and $c_{max}=0.9$. The reason for the larger resolution limit is the smaller total difference $\Delta\eta(Sn/Cu_6Sn_5)$. It is 0.038 in the 5 to 30 kV range, compared to 0.174 for gold over nickel, and 0.099 for tin over nickel. A similar plot for tin over Ni_3Sn_4 using 10% limits is given in Figure 17. $\Delta\eta(Sn/Ni_3Sn_4)$ is 0.030. In both cases the thickness estimates range from approximately from 0.006 to 0.58 μm (0.25 to 23 $\mu inch$). A correction factor of two, similar to that of tin over nickel, was applied for both.

Wear studies of contact surfaces are carried out frequently on gold or palladium over a nickel underplating. Gold over nickel

was used as a test system, and the results of a Monte Carlo simulation are given in Figures 8, 13, and 14. Such simulations were also performed for the system palladium over nickel. The results are given in Figure 18. The η_{min} and η_{max} for this system are given in the Figure 19.

Another application of the MCS/BSEIA technique is related to measurements of cross-sections. SEM BSE imaging of cross-sections is used to measure layer thickness too small to be resolved by optical microscopy. It is done by image analysis² of the phases visible in SEM BSE images of the cross section. Since the backscattered electrons are generated within a finite depth range at and below the surface, the BSE signal contains information from near-surface layers. The BSE signal depends

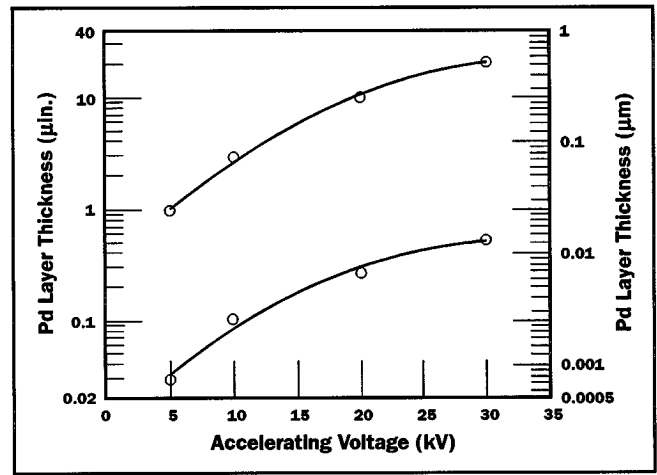
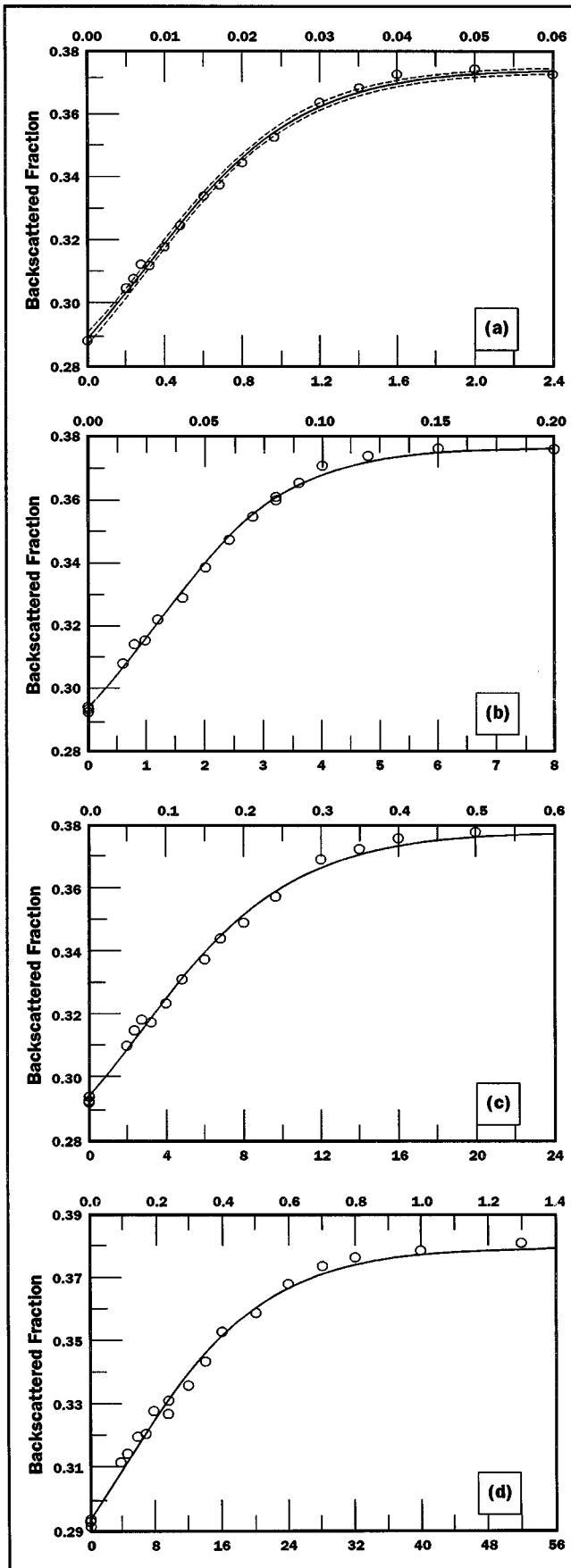


Figure 19. MCS/BSEIA detection limit, t_{min} , and saturation limit, t_{max} , versus accelerating voltage, for palladium layer on nickel substrate.

not only on the thickness of the layer but also on the accelerating voltage and certain material properties of the layer. They are its density and the atomic number of elements present. A special situation exists when a thin layer of one phase covers another phase. If the thin layer allows electrons to penetrate it, the BSE signal will be a mixture of electrons from both phases. For very thin layers the majority of the backscattered electrons come from the underlying phase, resulting in an overestimate of the true area occupied by this phase. For samples considered in this study, such a situation could occur at a tin/IMC interface because of the irregular nature of the IMC layer. To illustrate the effect, the cases of tin over Cu_6Sn_5 IMC and of Cu_6Sn_5 IMC over tin were considered. Figure 3c shows the variation of the backscattered fraction, measured at 20 kV, as function of the tin layer thickness applied to bulk Cu_6Sn_5 . In order not to favor one of the phases over the other the discrimination level must be set at $P_t=0.5$. At a thickness of about 0.3 μm (12 μinch) the BSE coefficient η is halfway between the bulk tin value and the bulk Cu_6Sn_5 value. Consequently, any area of tin over IMC with a tin layer thickness below 0.3 μm (12 μinch) will be considered an IMC area. Figure 20 shows the variation of the backscattered fraction as function of the Cu_6Sn_5 layer thickness over bulk tin; for this case the midway point is at about 0.25 μm (10 μinch). Any area with less than 0.25 μm (10 μinch) of Cu_6Sn_5 over tin will be considered a tin area. Thus, the effective sampling depth is relatively small and

Figure 18. Backscatter coefficient η versus thickness of palladium layer on nickel substrate at various values of the accelerating voltage 5 kV. Upper abscissa in μm , lower abscissa in μinch .—Points are Monte Carlo simulation, curve is sigmoidal fit; the dotted lines are confidence limits of the fit at 95% confidence level.—(a): 5 kV; (b): 10 kV; (c): 20 kV; (d): 30 kV.

nearly equal for both cases. Since a random cross-section will produce an equal incidence of both cases, the error resulting from the first case will be nearly equal and opposite the error from the second case, and the two will mostly cancel each other. For the above reasons, we do not expect a significant error due to the finite depth from which the backscatter electrons originate. The depth of information can be further reduced by using a lower accelerating voltage. In the 5 to 10 kV range it is similar to that for optical observation.

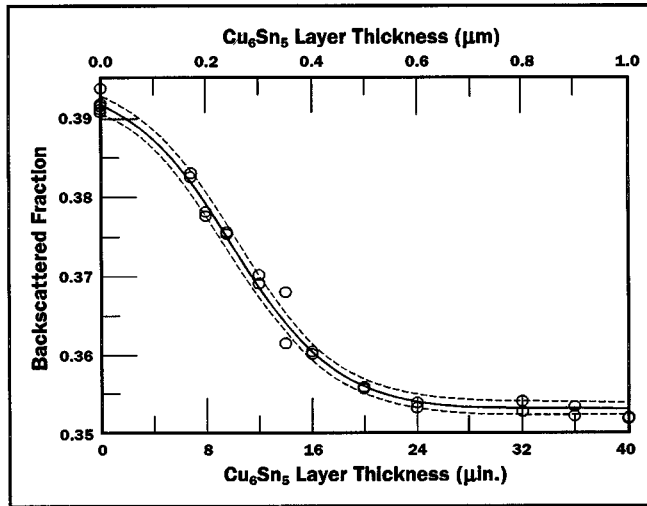


Figure 20. Backscatter coefficient η versus thickness of Cu_6Sn_5 layer on tin substrate, accelerating voltage 20 kV. Points are Monte Carlo simulation, curve is sigmoidal fit; the dotted lines are confidence limits of the fit at 95% confidence level.

DISCUSSION

Measurement of thin surface layers is inherently important for studies on contact surfaces. Such studies often require measurements of a large number of samples at high lateral resolution. The proposed technique, MCS/BSEIA, satisfies these requirements. It consists of the three elements: BSE imaging, image analysis, and Monte Carlo simulation of scattering from thin supported layers. None of the three individual components is new but they were not used in the combination and for the purpose described above. A number of researchers suggested use of BSE SEM for measuring film thickness⁸, or thickness and composition⁵. The suggested techniques use thickness and composition standards, but not simulation algorithms, to obtain the η_t versus thickness and η versus composition calibration curves. Although use of standards provides much better accuracy, the preparation of standards can be expensive and time-consuming. For compounds such as IMCs standards might not be easily available. The suggested techniques also do not use image analysis to analyze the backscatter data. Use of SEM BSE imaging has been suggested for measurements of small size particles⁹. This technique is similar to that described in this paper, but does not involve Monte Carlo simulation.

A user of the MCS/BSEIA technique has several options

- (a) use a series of standards,
- (b) use a small number of standards, one or two,
- (c) use no standards.

The standardless option (c) can speedily provide a reasonable estimate of thickness with no effort of making or obtaining standards. This was proven using the test specimens, tin on nickel and gold on nickel. Further improvements in the technique discussed above, such as a better Monte Carlo simulation program, or a BSE detector that collects a larger fraction of BSE electrons, will improve the estimates given by the technique.

A severe constraint on the implementation of this technique as applied in the present study is the necessity of having areas of the saturation thickness for substrate and coating materials in the same image frame as the areas of interest on the sample. This limits the range of applications for the technique. Stabilization of the instrumental output will eliminate this restriction by enabling sequential rather than simultaneous determination of the backscatter intensities of the substrate and coating materials.

SUMMARY

MCS/BSEIA is a fast and relatively inexpensive technique for estimating and/or measuring the thickness of thin surface layers in the approximate range of 0.003 to 1 μm (0.1 to 40 $\mu\text{in.}$), depending on the materials. The technique combines Monte Carlo simulation of the backscatter process with image analysis of backscattered electron image. The MCS/BSEIA method was confirmed by measurements of test samples of known thicknesses of tin and gold on nickel substrates. The technique was applied to measurement of surface area fractions of tin, lead, and IMC in aged tin and tin-lead platings. In these platings most of the tin was converted to an IMC and only a thin layer of tin remained at the surface. Other potential applications and improvements of the MCS/BSEIA technique were discussed.

ACKNOWLEDGEMENTS

The authors would like to thank Mr. Edwin Garver for plating test samples, Mr. Dennis Zerby for X-ray thickness measurements, and Dr. David C. Joy for supplying the Monte Carlo simulation program and for useful discussions on Monte Carlo simulation of the electron backscattering process.

REFERENCES

1. J. I. Goldstein, D. E. Newbury, P. Echlin, D. C. Joy, C. Fiori, and E. Lifshin, *Scanning Electron Microscopy and X-Ray Microanalysis* (Plenum Press, New York, 1981).
2. J. Haimovich, "Cu-Sn Intermetallic Compound Growth in Hot Air Leveled Tin at and below 100°C", *AMP J. of Technol.* **3**, 46-54 (1993).
3. D. C. Joy, "Monte Carlo Simulations of Electron Beam-

Solid Interactions," University of Tennessee, Knoxville, and Oak Ridge National Laboratory, Oak Ridge, 1992.

4. R. Hermann and L. Reimer, "Backscattering Coefficient of Multicomponent Specimens," *Scanning Electron Microsc.* **6**, 20 (1984).
5. D. J. Wilson and A. E. Curzon, "Film thickness and Composition Determination for Binary Alloys Using Backscattered Electrons," *Thin Solid Films* **165**, 217 (1988).
6. L. Reimer, *Scanning Electron Microscopy: Physics of Image Formation and Microanalysis* (Springer, Berlin, 1985).
7. G. E. Staudt, "Estimation of Uncertainty in Plate Thickness Measurement by X-ray Fluorescence," *AMP J. of Technol.* **3**, 85-97 (1993).
8. Y. Q. Sheng, P. Munz, R. Schultheis, and E. Bucher, "A Simple Method for Rapid Measurement of the Thickness of Ultrathin Metal Films," *Thin Solid Films* **131**, 131 (1985).
9. P. B. DeNee, "Measurement of Mass and Thickness of Respirable Size Dust Particles by SEM Backscattered Electron Imaging," *Scanning Electron Microscopy* **1**, 741 (1978).

Joseph Haimovich is a Member of Technical Staff in the Global Technology Group at AMP Incorporated, Harrisburg, Pennsylvania.

Dr. Haimovich holds a Dipl. Ing. degree in physical metallurgy from the St. Petersburg University in Russia and Master of Science and Ph.D. degrees in materials science from the University of Pennsylvania. Before joining AMP he worked in the fields of metallurgy of compound semiconductors and studied properties and structure of metallic glasses. His present area of expertise is metallurgy of solderable and contact coatings, particularly tin and tin alloy coatings. Dr. Haimovich published several papers on intermetallic compounds for connector materials and on mechanical properties and structure of metallic glasses. He is a member of ASM International and of The Minerals, Metals & Materials Society (TMS).

Kevin Leibold is an Analytical Chemist and the primary SEM operator in the Materials Engineering Department of the Global Technology Group of AMP Incorporated, Harrisburg, Pennsylvania.

Mr. Leibold holds a Bachelor of Arts degree with dual majors in Chemistry and Biology from Shippensburg University, Shippensburg, Pennsylvania. Since joining AMP in 1981 he has worked as an analytical chemist utilizing a variety of instrumental techniques. His present activities are focus on scanning electron microscopy including X-ray microanalysis and atomic spectroscopy.

Glenn E. Staudt is a Member of Technical Staff in the Global Technology Group at AMP Incorporated, Harrisburg, Pennsylvania.

Mr. Staudt received a Bachelor of Science degree in chemistry from Bucknell University, Lewisburg, Pennsylvania in 1974 and a Master of Arts degree in chemistry from Princeton University in 1976. From 1977 to 1981, he was employed as a chemist at Hamilton Technology, Inc. in Lancaster, Pennsylvania. Since joining AMP Incorporated in 1981, his activities have included technological support and research in the areas of electrodeposition and electrodeposited materials. Current research interests focus on the characterization of metallic coating systems.